Training Wall Effects on Power Generation of Tidal Stream Turbine Arrays Placed at Headlands

Andrea M. Schnabl
Department of Engineering Science, University of Oxford
Parks Road, Oxford, OX1 3PJ, UK
E-mail: andrea.schnabl@eng.ox.ac.uk

Thomas A. A. Adcock
Department of Engineering Science, University of Oxford
Parks Road, Oxford, OX1 3PJ, UK
E-mail: thomas.adcock@eng.ox.ac.uk

Guy T. Houlsby
Department of Engineering Science, University of Oxford
Parks Road, Oxford, OX1 3PJ, UK
E-mail: guy.houlsby@eng.ox.ac.uk

***Abstract*—Headlands are amongst the most promising features for potential tidal energy extraction sites, but the flow is significantly yawed with respect to the array plane. It has been suggested that guiding the flow has a positive impact on turbine loading and power production for this type of flow [1] [2]. This paper explores the effect of guiding the flow with training walls on power generation of a tidal turbine array at an idealised headland case [3] and a real site geometry, the Anglesey Skerries site, with realistic bathymetry and oscillating flow. The open-source code DG ADCIRC is used to solve the depth-averaged shallow water equations (SWEs) and a Linear Momentum Actuator Disc Theory (LMADT) model represents the turbines [4]. A parameter study is undertaken with the idealised headland site for both steady (constant flow rate) and unsteady flow conditions (sinusoidal water elevation). The parameters investigated in the study include shape, length, and angle of the training wall. Differences between steady and unsteady cases are explored for a range of flow rates (steady), frequencies and amplitudes (unsteady). The most favourable configurations are implemented in the real site simulation and compared to previous results without training walls.**

***Index Terms*—Tidal power, tidal stream turbine, resource assessment, headland, training wall**

I. Introduction

As the implications of climate change and the major contribution of fossil fuels to it are widely accepted now, a lot of effort is put in the development and deployment of renewable energy systems in order to limit green house gas emissions. Due to its predictability, tidal energy is a promising technology, especially in countries like the UK, which posses sites with high tidal range and fast tidal streams.

Tidal barrages have been installed since the 1960s, but due to their high capital costs and severe environmental impact, focus has been shifted to tidal stream technologies in recent years. Research on both the resource of sites and the specific siting of the turbines is still ongoing. Power optimisation is highly dependent on the turbine location, individual and with respect to others, and energy extraction influences the flow field, which in turn effects the available power. Analytical and numerical models have been developed to gain a better understanding of the underlying hydrodynamics and determine an upper bound for the resource at promising sites.

This paper discusses the effects of local blockage and so-called training walls on the available power at an idealised headland site and a real site. It has been suggested that guiding the flow with training walls results in a more efficient power extraction. This is investigated in this paper by looking at an idealised headland case and the effects of training walls with different lengths, shapes, and angles. The last part applies the results to a real site, the Anglesey Skerries headland, UK.

II. Related Work

In contrast to tidal channels, the flow at headland sites is unbounded on the ocean side. Therefore, power extraction is limited as the bypass flow around the array increases with increasing thrust [5]. In addition, the acceleration of the flow around the headland is accompanied by a diversion from the predominant flow direction far away from the headland. Belloni et al. (2013) suggest that bidirectional ducted turbines perform better in yawed flows than bare turbines, due to an increase in effective blockage and a flow accelerating and straightening effect of the duct [1]. Those effects could also be beneficial to turbine arrays placed off headlands with their highly yawed flow with respect to the turbine array. Therefore, extending this conclusion to the array scale, in this paper the duct is replaced with a training wall at the end of the turbine array.

The reasoning for this approach is reinforced by the findings of [2], who optimised the turbine micro-siting at several idealised sites and a real site, the Pentland Firth. The optimisation algorithm used in this work leads to rows of turbines, which are approximately perpendicular to the direction of the flow. An additional line of turbines is placed at either end of and perpendicular to these rows, funnelling the flow and retaining it inside the allotted site. The former rows extract the majority of the power, while a large part of the power generation of the latter rows is sacrificed for the mentioned funnelling purposes [2]. Instead of using turbines to guide the flow, training walls are used for this task in this paper.

While the geometry of the idealised headland in this paper is

taken from [3], Draper et al. (2012) and Neill et al. (2012) also investigated idealised headlands with different geometries [6] [7]. In addition to the idealised case [7] also considered tidal stream power generation at the Alderney Race, and [8] looked at the Portland Bill. However, the real site study in this paper is based on the work by [4].

III. Methodology

The DG ADCIRC model uses an LMADT turbine representation as a sub-grid model in a numerical SWEs model with a discontinuous Galerkin (DG) finite element method and a Runge-Kutta time discretisation [4]. Both experimental studies [9] and 3D RANS simulations [10] have shown qualitative agreement with the two scale LMADT model.

The investigation of the idealised headland is based on [3], who explored tidal farms at a headland in a wide channel. This analysis shows a fast current with a significantly large y-component around the tip of the headland, which makes it a perfect test case for the implementation of training walls [3].

Lastly, the final part of this work builds on the results of [4] for the Anglesey Skerries headland site. Both [3] and [4] used the DG ADCIRC model for their analysis. The DG ADCIRC code with an implemented LMADT turbine sub-grid model was selected for both the idealised headland and the real site. This code uses a discontinuous Galerkin finite element method to solve the shallow water equations. It is able to model discontinuities due to mass and momentum conservation for each individual element [11], and the elements are coupled by numerical fluxes [12]. Generally used fluxes are Roe's average flux, Lax-Friedrich flux, and HLL/HLLC flux [4], with the HLLC flux being used in the following simulations with DG ADCIRC.

A third-order explicit Runge-Kutta scheme in conjunction with a Courant-Friedrichs-Lewy (CFL) condition to account for its explicit nature is used for time discretisation.

IV. Numerical Simulations

A. Training Wall Effects at Idealised Headland

Due to its significantly yawed flow with respect to the array plane (meaning a considerable y-component of the flow velocity), training wall effects were studied at an idealised headland site as described by [3]. The domain consists of a wide channel (400 km length, 100 km width) and a headland of 20 km. The water depth around the headland is set to a constant 15 m, but increases to 1000 m further from the headland (as can be seen in Fig. 1), and a bed friction coefficient of 0.0025 was used, which is a typical value in analysis of tidal models [3].

The channel walls (boundaries B and D) were modelled as vertical walls with slip land boundaries, and the water level of boundary C was set to a constant 0 m. Additionally to the steady case (boundary A forced with constant, uniform upstream flow velocity of $u_0 = 0.02\ m/s$, $Fr_0 \approx 2 \cdot 10^{-4}$), a more realistic unsteady case was also studied. In this unsteady case, boundary A was forced by a sinusoidal tide with an amplitude of 2 m and a period of 12.42 h, resulting in a head difference across the length of the channel. A mesh convergence study was conducted until the difference in power was less than 2 %, which resulted in 3,294 nodes and 6,304 elements. The selected mesh is structured around the turbine array and unstructured everywhere else, as can be seen in Fig. 2. Element sides vary in length from around 40 m around the headland to around 10 km at the ends of the domain. To accommodate different angles of training walls, the mesh in the structured area had to be edited slightly for some of the simulations.

Fig. 1. Bathymetric depth

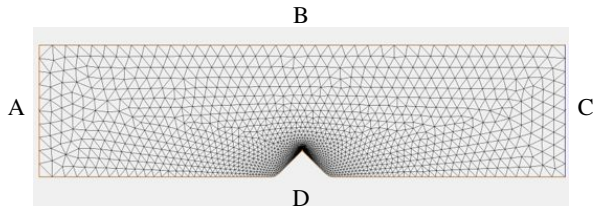

(a) Numerical mesh of the domain

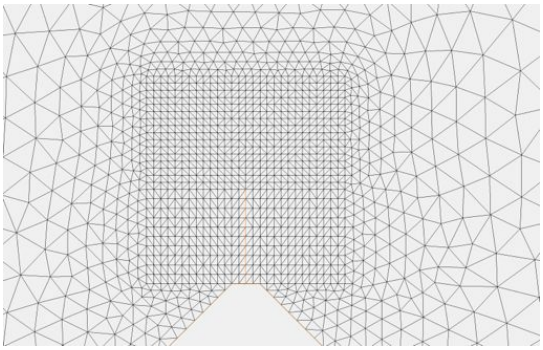

(b) Detail of the numerical mesh of the turbine array area

Fig. 2. Numerical mesh of the idealised headland

The turbine array extends 500 m into the channel, starting from the end of the headland, and the training walls were placed at the other end of the array. The local blockage was set to a relatively high value of $B_L = 0.4$ based on the mean water level for all cases. This value represents an upper bound for the practical range of local blockages and thus, for the power generation [13], but it is higher than that for the prototype devices currently being deployed. The parameter study included three different shapes of training walls:

1) straight line perpendicular to the turbine array (hereafter 'horizontal'),

2) straight line as an extension of the turbine array (hereafter 'vertical'),
3) v-shaped with the tip at the end of the turbine array (hereafter 'v-shape')

Schematic representations of all three types can be found in Fig. 3.

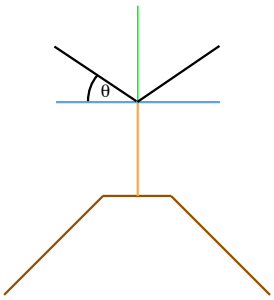

Fig. 3. Schematic representation of the training wall types: horizontal (blue), vertical (green), v-shape (black) situated at the end of the turbine array (orange)

In addition to the different shapes, the effect of the length of each of these training wall types was studied, with their length ranging from around 300 m to almost 1000 m. Four different wake velocity coefficients α_4 were simulated for each case, so that a cubic spline interpolation could be used to determine the maximum mean available power as explained by [13]. Available power in this context means available for power generation according to LMADT as opposed to total power extracted from the flow, which includes wake losses [14]. The effect of the different training wall shapes on the flow can be seen in Fig. 4, where the velocity in x-direction over the turbine array length is plotted for the undisturbed flow, a turbine array of 500 m without training walls, and the same array with each one of the three different shapes of training walls (horizontal, vertical, v-shaped).

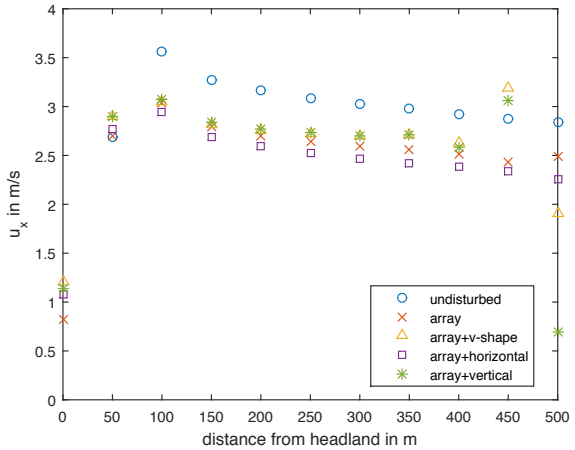

Fig. 4. Variation of the x-component of the velocity along the array length ($B_L = 0.4$, $l_{wall} \approx 500m$, $\alpha_4 = 0.5$, $Fr_1 \approx 0.26$)

The undisturbed flow velocity at the location, where later the array is placed, is highest relatively close to the coast (at a distance of 100 m) and drops slightly at larger distances. Including the turbine array lowers the flow speed across the entire length of the array compared to the undisturbed flow by approximately 14 % on average, while the general form of the distribution stays the same. Adding the horizontal training wall continues this trend. The velocities for the v-shaped training wall, on the other hand, are higher than the ones for the array alone, except for the very end of the turbine array (where the array connects to the training wall). At this point a drop in velocity can be observed. Right before this drop, another local maximum in velocity is reached, making the velocity profile more symmetrical. Given that the training wall in this case almost mirrors the headland coast, this was to be expected. The effect of the vertical training wall is very similar to the v-shaped one, with only significant differences at the maximum and drop at the far end of the turbine array.

Since the power scales with the third power of the flow velocity, Fig. 4 gives a good indication of the usefulness of the different training wall shapes. To explore this effect further and compare a range of lengths on the available power, a kinetic efficiency η_{kin}, similarly to the power coefficient C_P, was defined as:

$$\eta_{kin} = \frac{P}{0.5\rho A u^3}, \tag{1}$$

where P is the mean available power of the turbine array, A is the overall turbine area, and u is the average velocity at the array location in the undisturbed flow (i.e. without turbines or training wall present).

Using the normalisation according to Eq. 1, the different training wall shapes are compared to each other in Fig. 5. As was expected from the lower velocities in Fig. 4, the horizontal training wall actually reduces the available power. Even though the kinetic efficiency increases again with longer training wall lengths the original value (without a training wall) cannot be reached within the considered range of wall lengths. But the trend suggests a possible positive effect for even longer training walls.

On the one hand, both the vertical and the v-shaped training walls show a more favourable behaviour than the horizontal case. Both seem to follow the same trend, which again agrees well with the velocity distribution in Fig. 4. On the other hand, the total length of the combination of turbine array and training walls might be limited in some cases (e.g. due to shipping channels), so that the v-shaped training wall is more favourable than the vertical one as its vertical extent is shorter. The data in Fig. 5 shows a maximum around 750 m for the v-shaped training wall case and a drop in kinetic efficiency thereafter.

The large differences between the horizontal and the v-shaped/vertical shapes show that the angle of the training wall is of importance to its effectiveness. Therefore, a range of angles θ, as indicated in Fig. 3, was investigated. The v-

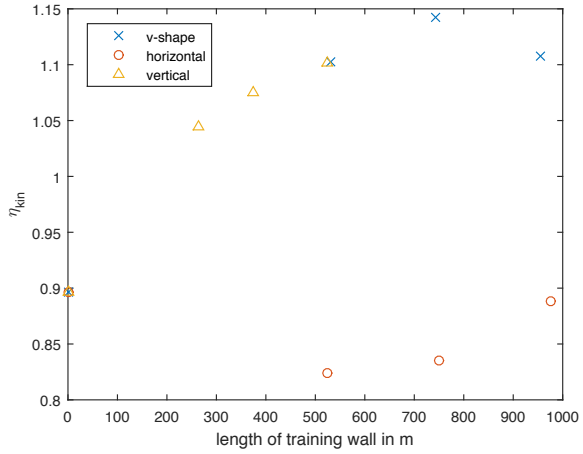

Fig. 5. Kinetic efficiency with respect to training wall length for different types of training walls ($B_L = 0.4$, $Fr_0 \approx 2 \cdot 10^{-4}$)

shaped training wall in the above discussed simulations had an angle of $\theta = 45°$. The results for a range of angles of $-10° \leq \theta \leq 30°$can be found in Fig. 6 for three different upstream flow velocities u_0 (forcing at boundary A):

case I: $u_0 = 0.02$ m/s (continuous lines in Fig. 6)
case II: $u_0 = 0.04$ m/s (dashed lines in Fig. 6)
case III: $u_0 = 0.01$ m/s (dash-dot lines in Fig. 6)

Tab. I lists the upstream flow velocity u_0, the spatially averaged velocity at the array location in the undisturbed flow $u_{1,av}$, and the Froude number at the array location in the undisturbed flow Fr_1.

TABLE I
FORCING AND FLOW DATA FOR DIFFERENT STEADY CASES

case	u_0 (m/s)	$u_{1,av}$ (m/s)	Fr_1
I	0.02	3.11	0.26
II	0.04	4.89	0.40
III	0.01	1.73	0.14

Both an increase in upstream flow velocity and in training wall length lead to a more efficient power extraction for the considered ranges. There is a clear maximum at an angle of around $\theta = 20°$. This maximum seems to be more pronounced at higher velocities and longer training walls, while it seems to move to larger values of θ for the low velocity/short training wall cases. In general, both a longer training wall and a higher angle θ lead to an increase in power as more of the flow is funnelled towards the turbine array. If θ is increased too much, the flow separates from the tip of the training wall and a recirculation zone forms below the downstream part of the wall, which leads to a decrease in power. Larger angles θ are still possible for slower flow velocities, as the flow can follow the contour of the training wall better, hence a slight shift of the optimum angle θ to higher values.

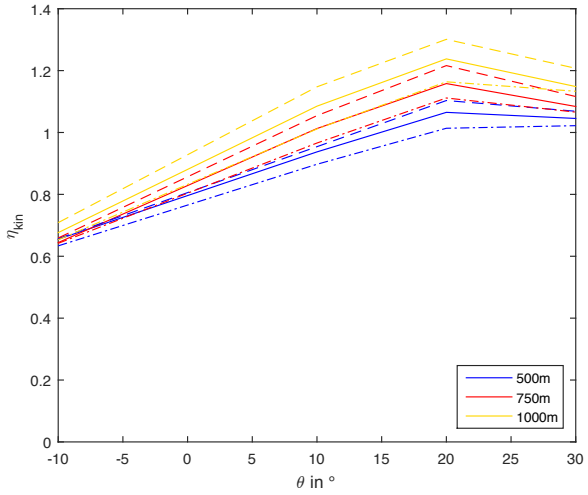

Fig. 6. Kinetic efficiency η_{kin} with respect to angle θ for different training wall lengths and different upstream velocities (continuous lines: case I, dashed lines: case II, dash-dot lines: case III)

Similarly, the shape of the headland can have a considerable impact on the power generation of the turbine array [6]. Therefore, it is highly likely that there is also a link between the optimum angle θ and the slope of the headland, i.e. the angle of the direction of the flow towards the turbine array. This possible correlation was further examined with a different headland shape with an aspect ratio of $\phi = 2$ (compared to the original one of $\phi = 1$). The results of this investigation can be seen in Fig. 7.

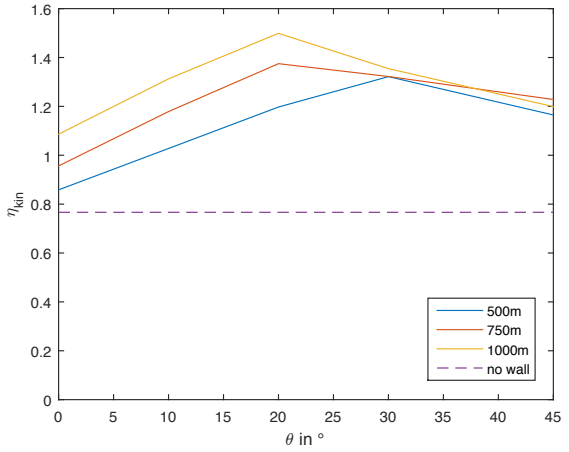

Fig. 7. Kinetic efficiency η_{kin} with respect to angle θ for different training wall lengths for a headland with aspect ratio $\phi = 2$ (steady)

The shift in optimum angle is even more evident for the headland with an increased aspect ratio. The increased incident angle between the incident flow and the horizontal tip of the headland leads to a flow separation at the leading edge of the headland. This results in streamlines that are almost parallel to the 'diffuser' part of the training wall and limits the flow separation at this point. A different shape of the training wall (e.g. comparable to the duct investigated by

[1]) might help mitigate these issues with flow separation at the inside of the training wall and improve the power generation further.

In the unsteady case, the available power changes periodically with the head difference across the channel length. In Fig. 8 an example of the available power over time in an unsteady case without a training wall is shown (blue line). It can be seen that even after the initial ramp up time two consecutive peaks do not reach the same value, which means that the flow is not symmetric, but the current is stronger in the direction right-to-left. Since the domain is symmetric, this behaviour was further investigated by exchanging the boundary conditions of the left and right boundaries, as well as imposing a sinusoidal elevation boundary with equal amplitudes (half of the original case) and frequency on both sides, but with a phase difference of π.

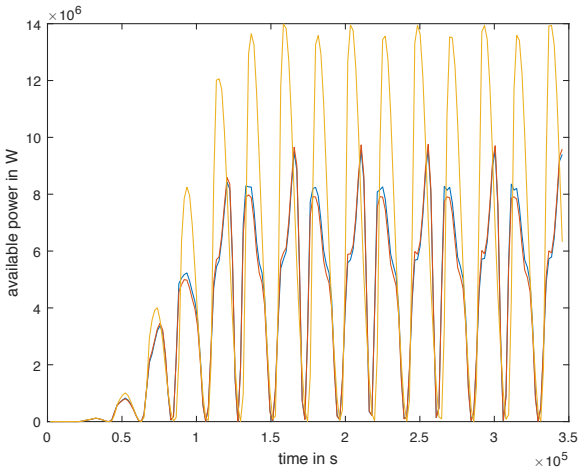

Fig. 8. Available power over time in unsteady case: sinusoidal forcing on the left (blue), right (red), and both boundaries (yellow)

As can be seen in Fig. 8, the two cases with the switched boundary conditions differ slightly, with the maximum deviation in power being less than 5 %. As power is proportional to the cube of the velocity, as small change in flow speed is magnified when looking at the power. The differences in velocity can be traced back to asymmetries in the mesh. However, the difference between these two curves and the one representing the forcing on both sides is significantly larger. This difference has been further investigated and it has been found that it is due to free surface effects. The mean water depth around the headland is only 15 m, so that there is a significant disparity in water depth for forcing with an amplitude of 2 m (forcing on one boundary) or 1 m (forcing on both boundaries). Linked to this water depth issue is a bed friction effect, as it is connected to the cube of the flow speed, which in turn is influenced by the water depth due to conservation of mass. The asymmetry between the two consecutive peaks can also be explained by the free surface effect, as the water depth at the array location is significantly lower for the flow direction right-to-left than for the opposite direction and thus, the flow speed increases.

Equivalent to Fig. 5 for the steady case, Fig. 9 shows the kinetic efficiency for the unsteady case. Here, u in Eq. 1 is chosen as the mean flow speed magnitude averaged over the array length in the undisturbed unsteady flow. This time the horizontal training wall has a positive effect and shows a maximum at around 750 m, before dropping again. In the case of the v-shaped training wall, the increase in power does not display an optimum value in the range of turbine lengths considered, whereas the vertical training wall type shows a maximum at around 400 m. As in the steady case, the effect of the v-shaped training wall on the power generation is more favourable than the other shapes. Therefore, this type will be used for further investigation and in the study of a real headland site, the Anglesey Skerries site.

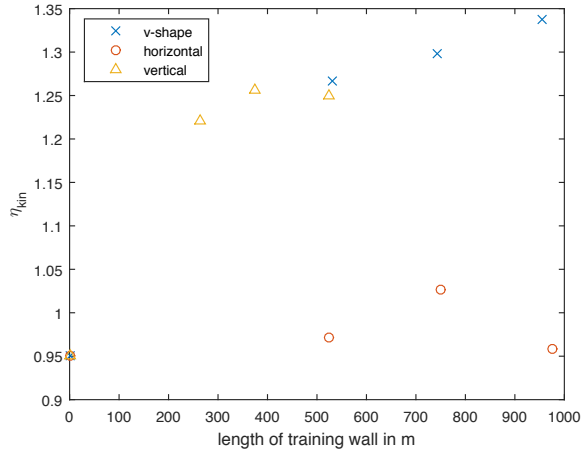

Fig. 9. Kinetic efficiency with respect to training wall length for different types of training walls ($B_L = 0.4$, unsteady)

The effect of the array and the training wall (here the v-shaped one) on the flow field can be seen in Fig. 10. The depth-average flow speed is shown for the area around the headland at peak current for: (a) no turbine arrays or training walls, (b) a turbine array of 500 m with local blockage of $B_L = 0.4$, (c) the same turbine array and a v-shaped training wall with $\theta = 45°$. The black arrows indicate the direction of the flow.

In Fig. 10 (a) the flow separating at the tip of the headland becomes apparent. A maximum flow velocity of about 2 m/s is reached and even though the kinetic energy flux is not a good measure for the upper or lower bound of the resource, it might be a potential indicator of promising sites [6] [3]. The flow field changes significantly, when a turbine array is added. The velocity after passing through the turbine array is slowed down due to the energy extraction, but the areas of both the accelerated bypass around the array on the ocean side and the decelerated wake downstream of the headland are increased. The v-shaped training wall increases the flow through the turbine array. At the same time it introduces a recirculation zone on its outer surface, leading to an increased

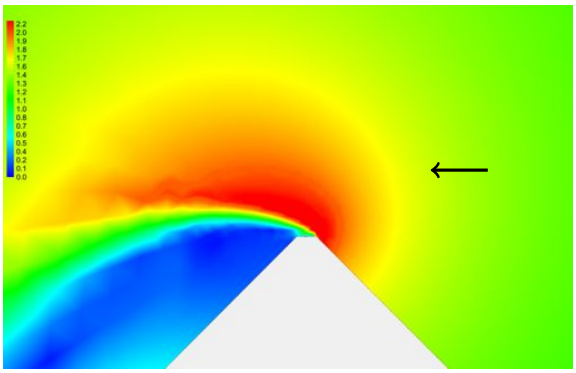

(a) Flowfield around headland

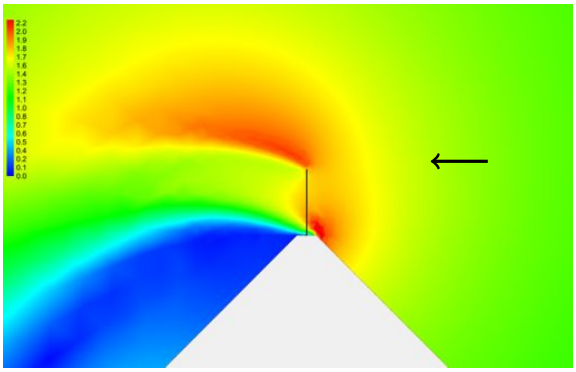

(b) Flowfield around headland with 500 m turbine array

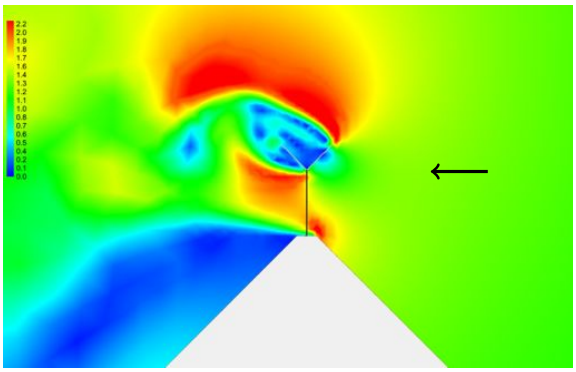

(c) Flowfield around headland with 500 m turbine array and 500 m v-shaped training wall ($\theta = 45°$)

Fig. 10. Depth-averaged velocity magnitude in m/s for unsteady case at peak current

energy dissipation and a lower basin efficiency as defined in [15].

Equivalent to the angle study for the steady case, a range of different angles θ was investigated for the unsteady flow conditions as well. The variation of the normalised power with the angle θ for several training wall lengths (500 m (blue), 750 m (red), 1000 m (yellow)) is plotted in Fig. 11. At real sites the tidal amplitude is contingent on the location and changes with the neap-spring cycle and the frequency depends on the dominant constituents at the considered location. Therefore, different forcing parameters (Fig. 11 (a) amplitude, Fig. 11 (b) frequency) have been considered similarly to the variation in upstream flow speed for the steady case. Tab. II lists forcing amplitude A, forcing period T, average velocity at the array location in the undisturbed flow $u_{1,av}$, and Froude number at the array location in undisturbed flow Fr_1.

TABLE II
FORCING AND FLOW DATA FOR DIFFERENT UNSTEADY CASES

case	A (m)	T (h)	$u_{1,av}$ (m/s)	Fr_1
IV	2	12.42	1.45	0.12
V a	4	12.42	2.08	0.17
V b	1	12.42	0.97	0.08
VI a	2	6.21	1.91	0.16
VI b	2	24.84	1.53	0.13

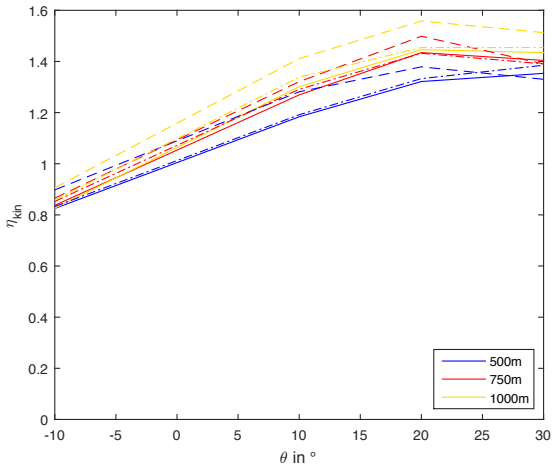

(a) Case IV (continuous lines), case V a (dashed lines), case V b (dash-dot lines)

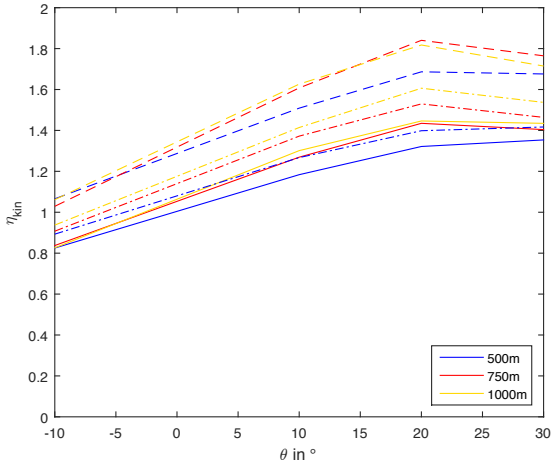

(b) Case IV (continuous lines), case VI a (dashed lines), case VI b (dash-dot lines)

Fig. 11. Normalised power with respect to angle θ for different training wall lengths and different forcing

The trends for the original forcing with an amplitude of $A = 2$ m and a period of $T = 12.42$ h (case IV; continuous lines in both plots) are comparable to the low speed steady case (case III), with an optimal θ of about 20°and a shift to larger angles for short training walls. For an even lower flow speed (case V b with $Fr_1 \approx 0.08$) the kinetic efficiency does not change significantly, except for an even more pronounced shift to a larger optimum angle. This was to be expected due to the low flow speed. The effect of the long training walls (750 m and 1000 m) at the optimum angle is very similar, which means added length does not lead to a significant increase in kinetic efficiency for this case.
Both a higher and a lower frequency of the sinusoidal forcing (dash-dot and dashed lines in Fig. 11 (a), respectively) lead to a higher kinetic efficiency, which can be linked to an increase in the average flow speed across the turbine array for both cases as shown in Tab. II. Nevertheless, the general trend with respect to θ remains unchanged. As the increase in kinetic efficiency for the 750 m long training wall even surpasses the longer one at the optimum and larger angles for the higher frequency case, there seems to be an optimum length in this case.

Again, these effects are highly likely to depend on the aspect ratio of the headland. Therefore, the unsteady case has been considered for the headland with the aspect ratio of $\phi = 2$ as well and the results are shown in Fig. 12.

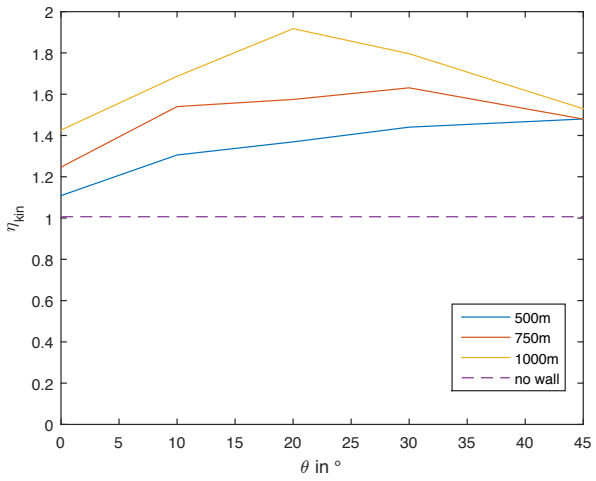

Fig. 12. Kinetic efficiency η_{kin} with respect to angle θ for different training wall lengths for a headland with aspect ratio $\phi = 2$ (unsteady)

Similarly to the steady case, the shift in optimum angle for shorter training walls is more noticeable than for the lower aspect ratio. Just like in the steady case, this is due to the limitation of the recirculation zone at the 'diffuser' part of the training wall as a result of the flow direction through the turbine array.
The environmental impact of turbine arrays at headlands due to a significant change in sediment transport was investigated by [7]. Moving the array offshore from the tip of the headland to limit these effects would result in a bypass flow between the headland and the array.

B. Training Wall Effects at Anglesey Skerries Site

Advancing from idealised sites to real coastlines and bathymetry, an existing model of the Bristol Channel and the Anglesey headland from [4] was modified. The mesh was slightly altered to accommodate a structured mesh for the turbine array and the training wall, as can be seen in Fig. 13. As a result of the study of the idealised headland, a v-shaped training wall was used.

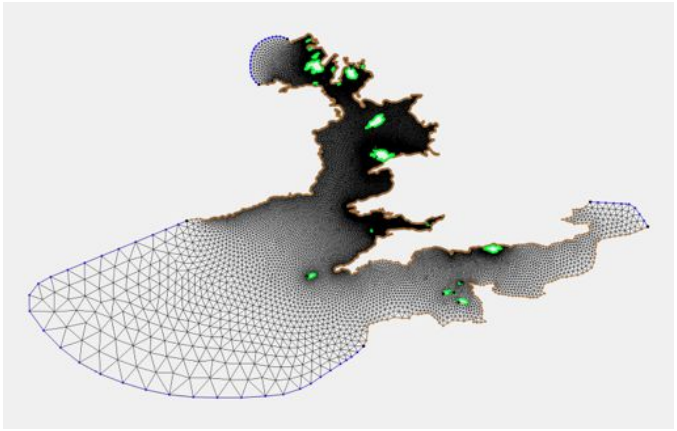

(a) Numerical mesh of the domain

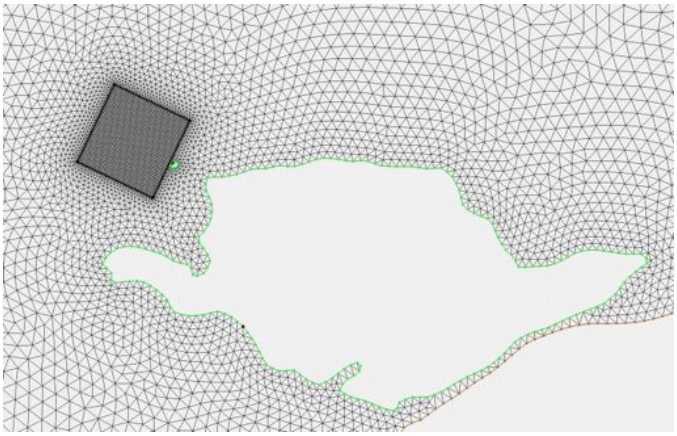

(b) Detail of the numerical mesh around the turbine array and training wall

Fig. 13. Numerical mesh of the Anglesey Skerries

The ASA2 case, a single array of turbines starting at the Skerries, with a local blockage of $B_L = 0.3$ in [4] was used as an example case here, since it was found to be one of the most favourable ones, while still having a reasonable local blockage. As far as possible the same or similar parameters as in [4] were used. Therefore, a turbine array of about 4.5 km length was implemented at approximately the same location, and the wake flow velocity coefficient α_4 was set to 0.39. A bed friction coefficient of 0.0025 was used. This value has been be determined during the validation of the model in the study by [4]. Following [4], the M_2 tide was the only tidal constituent used and was interpolated from the LeProvost

tidal database.

Table III shows a comparison between the results for the ASA2 turbine array itself and the ASA2 turbine array with a v-shaped training wall. In this table P_{avail} denotes the mean available power, P_{ex} the mean extracted power, and h_{av} the average water depth at the turbine array location.

TABLE III
COMPARISON OF ASA2 TURBINE ARRAY AT THE ANGLESEY SKERRIES HEADLAND SITE WITH AND WITHOUT TRAINING WALL

	P_{avail} (MW)	P_{ex} (MW)	h_{av} (m)
Serhadlıoğlu (2014)	70	122	36.3
Reproduction of Serhadlıoğlu (2014)	66	116	34.5
V-shaped training wall	114	199	34.5

Table III shows that the reproduction of the results from [4] agree reasonably well with the original study. Differences are mainly due to a slightly different turbine location, as can be seen from the average water depth column in the table. It can also be seen that the v-shaped training wall leads to an increase in available power of about 73 %. Even though this increase will certainly be smaller in reality, suggestions of a positive effect from guiding the flow seem to be true.

The wall in this case is around 4.5 km long, which means a substantial investment and environmental impact, as well as a significant increase in extracted power from the flow. But shorter walls already have a positive effect, with for example a length of 500 m leading to an increase in power of about 12 %, as can be seen in Fig. 14.

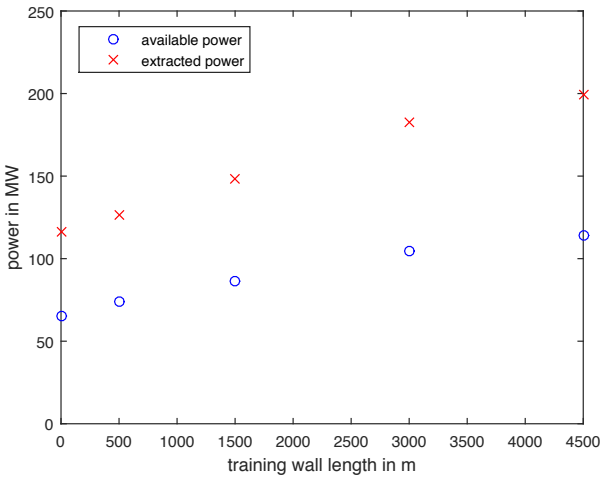

Fig. 14. Normalised available power and extracted power for a range of lengths (v-shaped training wall, 4.5 km long turbine array, $B_L = 0.3$)

The added effects of the training wall to the changes in the flow field around the Anglesey headland can be seen in Fig. 15, which shows the depth-averaged velocity for the headland with the 4.5 km long ASA2 turbine array and for an additional 3 km long training wall at the time of peak power.

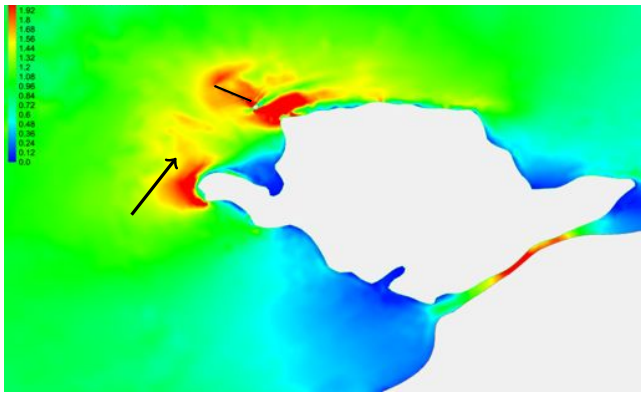

(a) Flowfield around a 4.5 km long turbine array

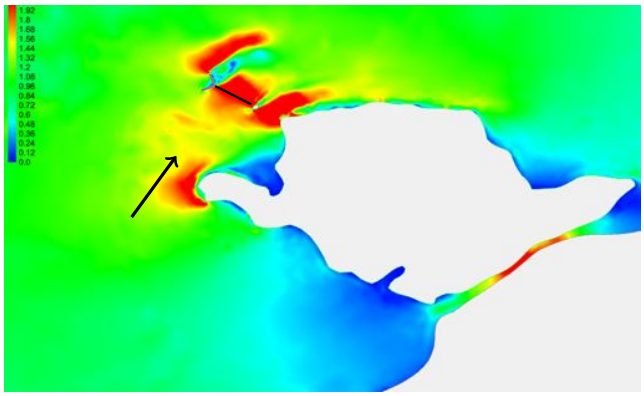

(b) Flowfield around a 4.5 km long turbine array and a 3 km long training wall

Fig. 15. Depth-averaged velocity magnitude in m/s around the Anglesey Skerries site at the time of peak power

The changes to the flow field are most pronounced around the turbine array. The funnelling effect of the training wall can be seen as the flow velocity through the turbine array is increased, which in turn leads to the increase in power. The bypass flow on the headland side is only slightly affected, while the bypass on the side of the open ocean changes drastically due to the training wall. The area, which was previously part of the bypass, is occupied by the training wall, so the accelerated flow around the array and wall is moved further towards the open ocean and it extends much further. This might lead to a change in, for example sediment transport. Therefore, additional attention has to be paid to cost and environmental concerns, finding a compromise between power generation and the mentioned problems. Moving on from the idealised headland case, further research is also needed in order to investigate the optimum shape and length of the training wall, as well as the influence of other parameters, for real sites.

V. CONCLUSION

In this paper, the influence of training walls for turbine arrays at idealised headlands has been investigated. The effect of training walls on the power generation has been examined

for different configurations of shape, length, and angle in an idealised headland site. An increase in power output due to the training wall has been shown for most of these configurations. Only horizontal training walls might have a negative effect, depending on length and flow conditions. When looking at a range of angles θ for the v-shaped training wall, an angle of $\theta = 20°$seems to be the optimum or close to the optimum for most of the explored variations in training wall length, upstream flow conditions, and tidal forcing. This is very convenient as flow conditions and tidal forcing at real sites are not as consistent as the idealised cases in this paper. But it has also been shown that larger angles are beneficial for lower flow velocities and/or headlands with larger aspect ratios, due to positive effects on the expansion of the recirculation area at the 'diffuser' part of the training wall in these cases.

A preliminary study of a real site, the Anglesey Skerries headland site, with regard to the effect of training walls has been conducted and an increase in power generation has been shown.

A limitation of this study is that shear profiles are neglected in the 2D model. The flow around headlands is complex and cannot be fully captured with a depth-integrated model [16], while the effect of training walls on the vertical profile is unclear. But according to [17] the change in normalised power due to shear profiles is small, assuming they are not too complex and the main objective of this paper is to discuss the leading order physics.

Further work is needed on the optimum configuration of training walls, including additional parameters, such as wall thickness and length of the turbine array. This study has indicated that it is difficult to optimise all of the various relevant parameters manually in order to improve power generation. Therefore, combining training wall material with an optimisation algorithm can help determine optimum structures with respect to these parameters and their interaction. The study of real sites, which was broached in Sec. IV-B, will be deepened and extended to other sites in future work.

REFERENCES

[1] C. S. K. Belloni, R. H. J. Willden, and G. T. Houlsby, "A Numerical Analysis of Bidirectional Ducted Tidal Turbines in Yawed Flow," *Marine Technology Society Journal*, vol. 47, no. 4, pp. 23–35, 2013. [Online]. Available: http://www.ingentaconnect.com/content/mts/mtsj/2013/00000047/00000004/art00004

[2] S. W. Funke, P. E. Farrell, and M. D. Piggott, "Tidal turbine array optimisation using the adjoint approach," *Renewable Energy*, vol. 63, pp. 658 – 673, 2014. [Online]. Available: http://www.sciencedirect.com/science/article/pii/S0960148113004989

[3] T. A. A. Adcock, "On tidal stream turbines placed off headlands," *Journal of Renewable and Sustainable Energy*, vol. 7, no. 6, 2015. [Online]. Available: http://scitation.aip.org/content/aip/journal/jrse/7/6/10.1063/1.4936361

[4] S. Serhadlıoğlu, "Tidal stream resource assessment of the Anglesey Skerries and the Bristol Channel," D.Phil. Thesis, University of Oxford, 2014.

[5] S. Draper, "Tidal Stream Energy Extraction in Coastal Basins," D.Phil. Thesis, University of Oxford, 2011. [Online]. Available: http://www.eng.ox.ac.uk/civil/publications/theses/theses%23tidal

[6] S. Draper, A. G. L. Borthwick, and G. T. Houlsby, "Energy potential of a tidal fence deployed near a coastal headland," *Philosophical Transactions of the Royal Society of London A: Mathematical, Physical and Engineering Sciences*, vol. 371, no. 1985, 2013. [Online]. Available: http://rsta.royalsocietypublishing.org/content/371/1985/20120176

[7] S. P. Neill, J. R. Jordan, and S. J. Couch, "Impact of tidal energy converter (TEC) arrays on the dynamics of headland sand banks," *Renewable Energy*, vol. 37, no. 1, pp. 387 – 397, 2012. [Online]. Available: http://www.sciencedirect.com/science/article/pii/S0960148111003855

[8] L. Blunden and A. Bahaj, "Initial evaluation of tidal stream energy resources at Portland Bill, UK," *Renewable Energy*, vol. 31, no. 2, pp. 121 – 132, 2006, marine Energy. [Online]. Available: http://www.sciencedirect.com/science/article/pii/S0960148105002193

[9] S. C. Cooke, R. H. J. Willden, B. W. Byrne, T. Stallard, and A. Olczak, "Experimental Investigation of Thrust and Power on a Partial Fence Array of Tidal Turbines," in *Proceedings of the 11th European Wave and Tidal Energy Conference*. EWTEC, 2015.

[10] E. Perez-Campos and T. Nishino, "Numerical validation of the two-scale actuator disc theory for marine turbine arrays," in *11th European Wave and Tidal Energy Conference (EWTEC 2015)*, 2015.

[11] E. J. Kubatko, S. Bunya, C. Dawson, J. J. Westerink, and C. Mirabito, "A Performance Comparison of Continuous and Discontinuous Finite Element Shallow Water Models," *Journal of Scientific Computing*, vol. 40, no. 1, pp. 315–339, 2009. [Online]. Available: http://dx.doi.org/10.1007/s10915-009-9268-2

[12] C. Eskilsson and S. J. Sherwin, "A triangular spectral/hp discontinuous Galerkin method for modelling 2D shallow water equations," *International Journal for Numerical Methods in Fluids*, vol. 45, no. 6, pp. 605–623, 2004. [Online]. Available: http://dx.doi.org/10.1002/fld.709

[13] T. A. A. Adcock, S. Draper, G. T. Houlsby, A. G. L. Borthwick, and S. Serhadlıoğlu, "The available power from tidal stream turbines in the Pentland Firth," *Proceedings of the Royal Society of London A: Mathematical, Physical and Engineering Sciences*, vol. 469, no. 2157, 2013. [Online]. Available: http://rspa.royalsocietypublishing.org/content/469/2157/20130072

[14] G. T. Houlsby, S. Draper, and M. L. G. Oldfield, "Application of linear momentum actuator disc theory to open channel flow," Department of Engineering Science, University of Oxford, Parks Road, Oxford, OX1 3PJ, U.K., Tech. Rep. OUEL 2296/08, 2008. [Online]. Available: http://www.eng.ox.ac.uk/civil/publications/reports-1/ouel_2296_08.pdf

[15] T. Nishino and R. H. J. Willden, "The efficiency of an array of tidal turbines partially blocking a wide channel," *Journal of Fluid Mechanics*, vol. 708, pp. 596–606, 10 2012. [Online]. Available: http://journals.cambridge.org/article_S0022112012003497

[16] P. K. Stansby, "Limitations of Depth-Averaged Modeling for Shallow Wakes," *Journal of Hydraulic Engineering*, vol. 132, no. 7, pp. 737–740, 2006. [Online]. Available: http://dx.doi.org/10.1061/(ASCE)0733-9429(2006)132:7(737)

[17] S. Draper, T. Nishino, T. A. A. Adcock, and P. H. Taylor, "Performance of an ideal turbine in an inviscid shear flow," *Journal of Fluid Mechanics*, vol. 796, p. 86112, 2016.